Crustal deformation and the seismic cycle across the Kodiak Islands, Alaska

Jeanne Sauber,[1] Gary Carver,[2] Steven Cohen,[1] and Robert King[3]

Received 12 January 2005; revised 16 September 2005; accepted 31 October 2005; published 8 February 2006.

[1] The Kodiak Islands are located ~120 to 250 km from the Alaska-Aleutian Trench and are within the southern extent of the 1964 Prince William Sound (M_w = 9.2) earthquake rupture and aftershock zone. Here we report new campaign GPS results (1993–2001) from northeastern Kodiak and reprocessed GPS results (1993–1997) from southwestern Kodiak. The rate and orientation of the horizontal velocities, relative to a fixed North America, range from 29.7 ± 1.7 mm/yr at N30.3°W ± 3.3°, located ~120 km from the deepest point of the trench, to 8.0 ± 1.3 mm/yr at N62.4°W ± 9.3°, located ~230 km from the trench. We evaluated alternate models of coseismic and interseismic slip to test the importance of the mechanisms that account for surface deformation rates. Near the Gulf of Alaska coastal region of Kodiak the horizontal velocity can be accounted for primarily by the viscoelastic response to plate motion and a locked main thrust zone (MTZ), downdip creep, and to a lesser extent, slip in the 1964 earthquake. Farther inland the dominant mechanisms that account for post-1964 uplift rates are time-dependent, downdip creep and a locked MTZ; for the horizontal velocity component, southwest translation of western Kodiak may be important as well. On the basis of the pre-1964 and post-1964 earthquake pattern of interseismic earthquakes, we suggest that between the occurrences of great earthquakes like the 1964 event, more moderate to large earthquakes occur in the southwestern Kodiak region than near northeastern Kodiak.

Citation: Sauber, J., G. Carver, S. Cohen, and R. King (2006), Crustal deformation and the seismic cycle across the Kodiak Islands, Alaska, *J. Geophys. Res.*, *111*, B02403, doi:10.1029/2005JB003626.

1. Geologic and Tectonic Setting

[2] The motion of the Pacific plate relative to the North American plate (PCFC-NOAM) is at a rate of about 57 mm/yr at N22°W [*DeMets et al.*, 1994; *DeMets and Dixon*, 1999] near the Kodiak Islands (hereafter the main Kodiak Island and the islands of the surrounding region will be referred to as "Kodiak"). Kodiak spans a region approximately 120 to 250 km from the Alaska-Aleutian Trench (taken here to be the deepest bathymetric contour which ranges from 4000 m to 5200 m, Figure 1). The subducting Pacific plate is thought to have a shallow dip (<10°) from the Aleutian trench northwestward to 30–40 km below Kodiak based on seismicity [*Davies et al.*, 1981; *Pulpan and Frohlich*, 1985] and the geological structure suggested from a deep crustal transect [*vonHuene et al.*, 1999]. From the northeastern to the southwestern part of the island the distance from the Aleutian trench to the coast of Kodiak narrows by about 10% (Figure 1). This change probably reflects a slight steepening of the dip of the down going Pacific plate under the southwestern part of the island.

[3] All of Kodiak lies within the southern extent of the 1964 Prince William Sound (M_w = 9.2) earthquake rupture and aftershock zone. Prior to the 1964 earthquake, in 1900, a M_S = 7.7 earthquake occurred in the southeastern part of Kodiak [*Gilpin et al.*, 1994; *Gilpin*, 1995; D. I. Doser et al., personal communication, 2004]. *Nishenko and Jacob* [1990] suggest a recurrence interval of ~60 years between periods of increased activity that last as long as 10 years based on large and great earthquakes felt on Kodiak during the last 200 years; they considered all of the Kodiak as one segment of the Alaska-Aleutian subduction zone. Recently, several large earthquakes (M_w = 7.0, in 1999; M_w = 6.5 in 2000; M_w = 7.0 in 2001) have occurred in the southwestern part of the Kodiak as well [*Ratchkovski and Hansen*, 2001; *Hansen and Ratchkovski*, 2001]. The Harvard and U.S. Geological Survey (USGS) centroid moment tensor solutions (CMTs [*Dziewonski and Woodhouse*, 1983; *Ekström*, 1994; http://neic.usgs.gov/neis/sopar]) for the events are given in Figure 1. The focal mechanisms of earthquakes that occurred between November 1977 and February 2004 indicate a combination of reverse faulting events on northeast-southwest striking planes and left-lateral strike-slip events at roughly trench-parallel orientations (Figure 1). These earthquakes, as well as earthquake focal mechanisms from 1964 to 1979, are discussed in relation to the 1964 earthquake by *Doser et al.* [2002]; they found that the

[1]Planetary Geodynamics Laboratory, NASA's Goddard Space Flight Center, Greenbelt, Maryland, USA.
[2]Department of Geology, Humboldt State University, Arcata, California, USA.
[3]Department of Earth, Atmospheric, and Planetary Science, Massachusetts Institute of Technology, Cambridge, Massachusetts, USA.

0148-0227/06/2005JB003626$09.00

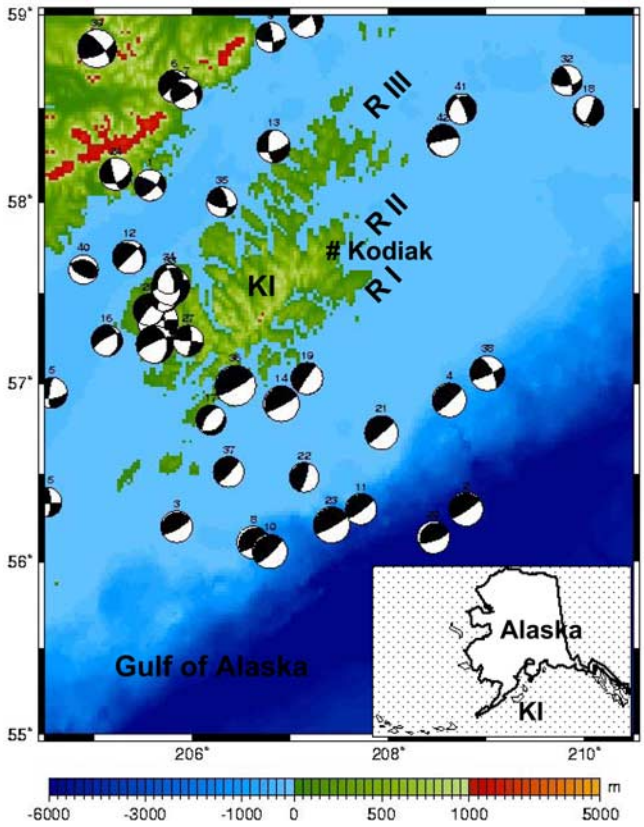

Figure 1. Topography and focal mechanisms from the Kodiak Islands and the surrounding region. The focal mechanisms were derived from Harvard centroid moment tensor and USGS fast moment tensor solutions (1977–2004 [*Dziewonski and Woodhouse*, 1983; *Ekström*, 1994; http://neic.usgs.gov/neis/sopar]). The earthquake location, fault plane parameters, and date are given in Table 5. The topography (SRTM30_PLUS, http://topex.ucsd.edu/WWW_html/srtm30_plus.html) is based on SRTM data discussed by *Farr and Kobrick* [2001] and seafloor topography from *Smith and Sandwell* [1997]. The topography and focal mechanisms were plotted using the program iGMT [*Becker and Braun*, 1998]. KI, Kodiak Island; number Kodiak, the city of Kodiak. The longitude is given in °E. The location of Kodiak Island on an outline of the state of Alaska is given in the bottom right-hand corner. R I, region I: Gulf of Alaska coastal regions includes Narrow Cape fold and thrust belt, the Narrow Cape fault, and along the western boundary of R I, the Kodiak Island fault (Figure 2). R II, region II, Late Cretaceous Belt. This central region appears to have uplifted more rapidly than the region northwest of the Border Ranges fault (Figure 2) resulting in a northwest tilt of the islands [*Gilpin*, 1995]. R III, region III, this region of volcanic arc basement forms a backstop northwest of the Border Ranges fault (BR). The degree of lithification generally increases from southeast to northwest across the island [*Gilpin*, 1995].

earlier earthquakes between 1964 and 1979 were characterized by more normal and normal-oblique mechanisms. The earthquakes since 1964, as well as historical earthquakes reported by *Gilpin* [1995], indicate that southwestern Kodiak has had moderate to large earthquakes more frequently than northeastern Kodiak both prior to, and following, the 1964 earthquake.

[4] The Kodiak Islands are part of a large subduction complex that comprises the eastern Aleutian forearc; the islands form the subaerial part of a broad topographic ridge that includes a Mesozoic-Cenozoic accretionary complex (Figure 1). The Kodiak Seamount (24 Ma) is part a hot spot chain that transects the Gulf of Alaska; it is the oldest seamount still exposed prior to subduction. *VonHuene et al.* [1999] hypothesized that a thickened and thermally hot oceanic crust in this region is a more buoyant segment than adjacent crust and may have acted as a second seismic asperity in the 1964 earthquake (the primary asperity and epicenter was in the Prince William Sound area).

[5] In section 2, we report horizontal velocities and uplift rates estimated from GPS measurements made between 1993 and 2001 across the northeastern region of Kodiak Island. To put these results in a regional context, we included in our analysis GPS measurements made by *Savage et al.* [1999] across the southwestern Kodiak and measurements from the two permanent stations (KOD1 and KODK). We used the two-dimensional (2-D) plane strain finite element model (FEM) TECTON [*Melosh and Raefsky*, 1981] to estimate the predicted surface displacements due to coseismic slip, interseismic strain, and alternate postseismic deformation mechanisms. Additionally, we explored the importance of mechanisms not easily modeled with the 2-D FEM model by using elastic dislocation models [e.g., *Savage*, 1983]. We used the geodetic results and the model predictions to further address the following questions: (1) How do the ongoing crustal deformation rates vary as a function of distance from the trench and as a function of time since the 1964 earthquake? (2) Are there mechanisms other than plate motion and a locked MTZ needed to account for the geodetic results? (3) What was the magnitude of 1964 coseismic slip near northeastern and southwestern Kodiak? (4) What is the seismic history of moderate to large earthquakes and are there differences between these two regions?

2. Global Positioning System Measurements and Analysis

[6] To estimate station velocities, we have used observations from eight locations on Kodiak Island acquired with varying occupation scenarios between 1993 and 2001 (Table 1), along with observations from the two Kodiak permanent GPS stations. We surveyed five primary stations in the northeastern part of the island (PASA, MILB, CLAM, KODI, and SKI0) three or four times between 1993 and 2001, occupying most of these for 6–8 hours on 1–4 days but KODI continuously for the length of each survey. In 1995, 1997, and 1999 these observations were made as part of an education outreach program with Kodiak Island High School [*Stockman et al.*, 1997; *Sauber et al.*, 1998]. There are two extended "geodetic footprints" in our northeastern Kodiak geodetic network (Table 1). The KODI footprint includes a station, KODV (10 m from KODI), that was previously measured with very long baseline interferometry (VLBI) between 1984 and 1990 [*Ma et al.*, 1990]. The footprint also includes the permanent station KODK (located

Table 1. Site Location and Observation History

Station	Abbreviation	Latitude, °N	Longitude, °W (°E)	1993[a]	1995[a]	1997[a]	1998[a]	1999[a]	2000[a]	2001[a]	2002[a]	2003[a]
Sitkink[b]	SITK	56.54	−154.14(205.86)	3	2	4	0	0	0	0	0	0
Pasagshak	PASA	57.44	−152.46(207.54)	0	0	3	0	2	0	1	0	0
Eastern Coast, Kodiak DGPS Site, KOD1, and Extended Footprint												
Kodiak DGPS	KOD1	57.62	−152.19(207.81)	0	0	27	3	7	10	6	6	5
Chiniak	CHIN	57.62	−152.16(207.84)	0	3[c]	1[c]	0	0	0	0	0	0
Miller FieldA	MILA	57.61	−152.20(207.80)	0	1[c]	0	0	0	0	0	0	0
Miller FieldB	MILB	57.62	−152.19(207.81)	0	2[c]	1[c]	2	3	0	0	0	0
Akhiok[b]	AHKI	57.94	−154.17(205.83)	4	1	3	0	0	0	0	0	0
Clam	CLAM	57.65	−152.51(207.49)	0	3[c]	2	0	3	1	0	0	0
Kodiak Fiducial and Extended Footprint Near Town of Kodiak												
Kodiak RM2	KODI	57.74	−152.50(207.50)	13[d]	27[d]	4[d]	3[d]	6[d]	1	1	0	0
Kodiak IGS	KODK	57.73	−152.50(207.50)	0	0	0	0	0	10	11	6	0
Kodiak VLBI	KODV	57.74	−152.50(207.50)	1	1[c]	0	0	0	0	0	0	0
NOAA Vertical	NOAA	57.73	−152.50(207.50)	0	0	0	0	0	2	0	0	0
Ski Challet	SKI0	57.80	−152.61(207.39)	0	4[c]	1[c]	0	2	0	2	0	0
Karluk[b]	KRLK	57.56	−154.45(205.55)	3	2	3	5	0	0	0	0	0

[a]Number of observation days; KODK, KOD1, 24 hours; KODI, AHKI, SITK, KARL, 7–24 hours; others, 3–8 hours.
[b]Katmai network of *Savage et al.* [1999].
[c]Trimble L1/L2 antenna; otherwise, choke ring antenna.
[d]Spike mount; otherwise, tripod setup.

within 1 km of KODI) constructed in late 1998 as part of an educational and outreach program with NASA's Goddard Space Flight Center, Kodiak Island High School, and Thales Navigation. The second extended footprint includes our station MILB located near the U.S. Coast Guard station KOD1, installed in 1997 as a Continuously Operating Reference Station (CORS) of the National Geodetic Survey. Additional nearby stations within the two footprints were surveyed once or twice for back-up in case the primary site was destroyed (Table 1).

[7] The U.S. Geological Survey (USGS) surveyed three stations (KRLK, AHKI, SITK) in the southwestern part of Kodiak as well as additional stations on the Alaska Peninsula in 1993, 1995, and 1997, occupying each station for at least 48 hours [*Savage et al.*, 1999]. The southwestern Kodiak stations were surveyed again in 2001 by the USGS. However, since there were large nearby earthquakes between 1999 and 2001, we used only the Kodiak observations through 1997 in our analysis.

[8] We obtained the velocities of the GPS stations using the GAMIT/GLOBK software [*King and Bock*, 2003; *Herring*, 2003] and the procedure described by *McClusky et al.* [2000], combining the observations from our field receivers with those of the global IGS network processed at the Scripps Orbit and Permanent Array Center (SOPAC) [*Bock et al.*, 1997]. To define a North America reference frame, we minimized the horizontal velocities of 11 stations within the nondeforming regions of the North America and Pacific plates (Table 2). The residual motion of these 11 stations is 0.8 mm/yr.

[9] In order to evaluate the uncertainties of our velocity estimates, we computed and examined time series of position within each survey and over the full span of our data for stations with at least three observation time periods (see position plots in the auxiliary material[1]). With the a priori uncertainties we assigned to the phase observations, the normalized RMS of the long-term repeatability has a median value of about 0.7, which we have found from analysis of similar but more extensive data sets to result in realistic uncertainties in velocities estimated from 2 or more years of observations [see, e.g., *McClusky et al.*, 2000]. For those stations in the Kodiak network whose unscaled NRMS scatters were greater than 1.0 we down-weighted the position estimates to achieve values closer to 0.7. Our estimates of vertical motions are less reliable than those for horizontal motion in part because of larger uncertainties in the estimates of height from the short observation scenarios used for many of the surveys and in part because of larger vertical uncertainties in reference frame.

[10] The estimated velocities and uncertainties for Kodiak and plate-defining stations are given in Tables 2 and 3 in our North America frame. The well-determined horizontal velocities for the Kodiak are shown in Figure 2. Velocities for all the stations in our solution, in both the North America and ITRF2000 (no net rotation) frame, may be found in the electronic supplement. With respect to the Pacific plate, all of the velocities in the region have an additional uncertainty of 1.0 mm/yr in magnitude and 0.7 deg in azimuth due to the uncertainty in our estimate of the rotation vector between the North America and Pacific plates.

[11] We have a small number of stations located within extended footprints to assess the internal consistency of the velocities. The stations within the individual KOD1 and KODI footprints have similar horizontal velocities within the 1σ level of uncertainty (Table 3 and the auxiliary material); the vertical uplift rates, however, show greater variability. From a solution in which the estimated vertical rates of the nearest North American stations (at Penticton, British Columbia, and Fairbanks) are less than 3 mm/yr, we estimated uplift rates of −2 to 19 mm/yr with uncertainties of about 5 mm/yr. There is an apparently consistent pattern, however, with stations 120–150 km from the trench (SITK and KOD1) showing ~10 mm/yr less uplift than stations 170–230 km from the trench (CLAM/KODI/KODK/SKI0/

[1]Auxiliary material is available at ftp://ftp.agu.org/apend/jb/2005JB003626.

Table 2. North America Fixed Reference Frame Stations[a]

Station	North Rate, mm/yr	N_σ, mm/yr	East Rate, mm/yr	E_σ, mm/yr	Vertical, mm/yr	V_σ, mm/yr
			North American Stations			
STJO	0.82	0.86	−0.22	0.87	−0.28	0.87
BRMU	0.70	0.62	0.15	0.63	−1.42	0.85
ALGO	−0.33	0.63	0.25	0.64	2.98	0.73
NLIB	0.50	0.32	0.53	0.34	−1.14	0.82
MDO1	0.11	0.30	−0.37	0.33	0.23	0.82
PIE1	−0.25	0.78	−0.26	0.80	2.08	0.80
YELL	−0.44	0.25	0.38	0.25	3.86	1.13
WILL	0.78	0.98	−0.08	1.00	−0.08	1.27
			Pacific Plate Stations			
CHAT	52.87	0.89	−38.22	0.88	1.14	1.30
KWJ1	47.17	1.13	−69.44	1.33	−3.76	2.86
MKEA	51.62	0.87	−59.75	0.91	−2.67	2.83

[a]The correlation between components of less than 0.03.

KRLK). Though less reliable than the horizontal velocities, the GPS estimate of vertical rates in conjunction with VLBI and tide gauge measurements do provide useful constraints on some of our models.

[12] Earlier space-geodetic results can be compared to our velocity results as well. VLBI measurements were made on the USGS base near the city of Kodiak between 1984 and 1990 [*Ma et al.*, 1990]. In a NUVEL-1 North America fixed reference frame a horizontal rate of 10.4 ± 1.0 mm/yr at N40.1°W ± 5.4° and an uplift rate of 14.0 ± 7.2 mm/yr were estimated for the VLBI data [*Ryan et al.*, 1993]. The VLBI horizontal velocity and vertical uplift rate are within 1σ of the GPS results for KODI (Table 1), a monument located 10 m from the old VLBI monument.

3. Trench-Parallel and Plate-Normal Components of Slip

[13] The map view of the horizontal velocities given in Figure 2 and the orientations given in Table 3 illustrate the counterclockwise rotation of the velocity vectors for stations farther from the trench (especially KRLK, SKI0, KODI) relative to stations near the eastern coast of Kodiak Island (SITK, PASA, KOD1). To explore the implications of this change in orientation, we rotated the horizontal station velocities to be plate parallel and plate normal as well as trench normal and trench parallel (Table 3). As mentioned earlier the motion of the Pacific plate relative to the North American plate (PCFC-NOAM) is at a rate of about 57 mm/yr at N22°W [*DeMets et al.*, 1994; *DeMets and Dixon*, 1999] in this region.

[14] A discrepancy between the relative plate motion direction and the trench normal could result in oblique slip on the plate interface or partitioning of slip between dip slip on the downgoing plate interface and strike slip on upper crustal faults [see, e.g., *McCaffrey et al.*, 2000, and references therein] On the basis of earlier modeling of coseismic slip in the 1964 earthquake, we assumed interface slip to be primarily dip-slip motion. Since there is a difference between the trench normal (N35°W) and the direction of PCFC-NOAM motion (N22°W), right-lateral slip is predicted (Table 3), but has not been observed in the field, on trench-parallel, upper plate faults.

[15] The velocities of the coastal stations (SITK, PASA, KOD1) have orientations that are close to the trench normal of N35°W, but are actually between the plate direction and the trench normal (Table 3). For the northeastern and southwestern Kodiak stations, the trench-normal (N35°W) velocity component decreases nearly uniformly with distance from the trench (Figure 3) as would be expected if this velocity component is associated with a locked main thrust zone primarily offshore (toward the trench). These results are the subject of section 4. Here we discuss the trench parallel (N55°E) or plate normal (N68°E) velocity compo-

Table 3. Geodetic Site Velocities in a North American Fixed Reference Frame and the Site Velocities Resolved Into Plate-Parallel (N22°W), Plate-Normal (N68°E), Trench-Normal (N35°W), and Trench-Parallel (N55°E) Components

Site Name	Distance From Trench, km	Horizontal Rate ± σ, mm/yr	Orientation ± σ , deg	Vertical ± σ, mm/yr	Rate, mm/yr			
					N22°W	N68°E	N35°W	N55°E
SITK[a]	120.	29.7 ± 1.7	N30.3W ± 3.3	−2 ± 4	29.4	−4.3	29.6	2.4
PASA	147.	25.3 ± 1.4	N32.9W ± 4.2	8 ± 10	24.8	−4.8	25.3	0.9
KOD1	153.	17.6 ± 2.1	N28.8W ± 6.8	6 ± 2	17.5	−2.1	17.5	1.9
MILB	153.	18.5 ± 1.8	N20.8W ± 5.5	16 ± 5	18.5	0.4	17.9	4.5
AHKI[a]	159.	19.1 ± 2.2	N33.5W ± 6.6	2 ± 5	18.7	−3.8	19.1	0.5
CLAM	172.	14.0 ± 1.3	N39.5W ± 5.5	17 ± 3	13.4	−4.2	13.9	−1.1
KODI	182.	11.3 ± 1.5	N49.3W ± 7.7	14 ± 4	10.0	−5.2	10.9	−2.8
KODK	182.	13.5 ± 1.6	N48.3W ± 6.7	9 ± 5	12.1	−5.9	13.1	−3.1
SKI0	192.	8.5 ± 1.0	N59.7W ± 6.5	12 ± 3	6.7	−5.2	7.7	−3.5
KRLK[a]	228.	8.0 ± 1.3	N62.4W ± 9.3	19 ± 4	6.1	−5.2	7.1	−3.7
NUVEL-1A[b]					57.	0.0	55.5	12.8

[a]Katmai network of *Savage et al.* [1999].
[b]Predicted Pacific plate motion relative to stable North America.

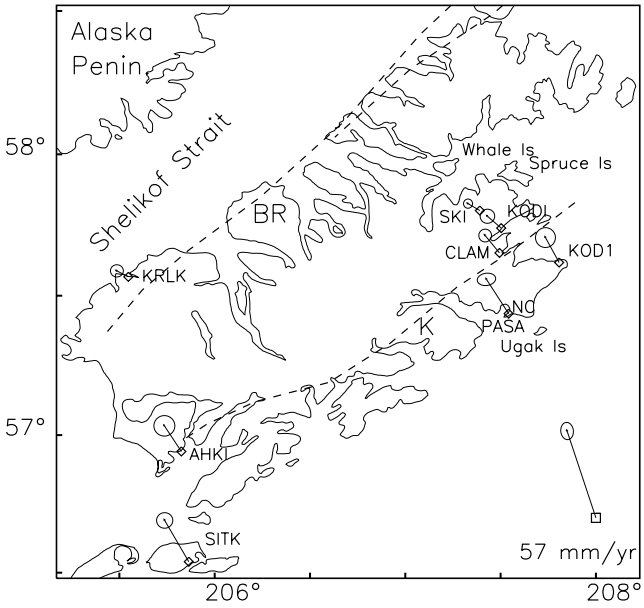

Figure 2. Map showing representative GPS station velocities from the northeastern Kodiak network (Table 3) and the southwestern Kodiak stations from the Katmai network [*Savage et al.*, 1999] with our computed horizontal velocity and 95% confidence error ellipses. BR, Border Ranges; K, Kodiak Island fault; NC. Narrow Cape; and SKI, SKI0 in Table 1.

nent in the context of other regional geodetic results and field geologic measurements from northeastern Kodiak Island.

[16] Site velocities derived from GPS measurements from south central, coastal Alaska (between Yakutat and Cordova) indicate a more westerly orientation (N27°W) than that predicted by the PCFC-NOAM (N12°W) as well [*Savage and Lisowski*, 1988; *Sauber et al.*, 1997, 2000]. Their models included virtual dip slip on the MTZ and strike slip at the base of the locked MTZ. In contrast to the Kodiak region, however, the velocity component perpendicular to the plate motion direction decreased at sites located farther inland.

[17] On Kodiak, the trench parallel component of velocity shown in Table 3 suggests shear strain that would be released as left-lateral strike-slip motion on upper plate faults; this would result in southwest motion of the western Kodiak Island. In contrast, slip partitioning of the PCFC-NOAM plate motion would predict right-lateral slip and clockwise rotation of the stations inland from the locked main thrust zone (see trench-parallel component of NUVEL-1, Table 3). The Kodiak Island and Narrow Cape faults are the largest mapped approximately trench-parallel faults in this region. Mapping and paleoseismic studies of the Narrow Cape fault show it has produced predominately left-lateral strike-slip displacement during the Holocene [*Carver et al.*, 2003]. The paleoseismic results are consistent with the geodetic results.

[18] Velocities of GPS sites on Unimak and Sanak islands, the Shumagins, and the Alaska Peninsula show displacement rates of ~4 mm/yr to the southwest [*Freymueller and Beavan*, 1999; *Mann and Freymueller*, 2003]. Since there was little indication of strain associated with the subduction earthquake cycle (trench normal motion), they interpreted these velocities to indicate southwest translation of those regions relative to North America. They hypothesized that this could result from any of three mechanisms (1) motion of the Bering Sea microplate; (2) translation of a large section of southern Alaska on the Denali fault system; or (3) translation of a forearc/arc sliver resulting from oblique subduction [*Mann and Freymueller*, 2003, and references therein]. In the next section we focus on modeling of the surface deformation associated with the subduction plate interface.

4. Modeling of Kodiak Island Geodetic Observations

[19] Although the epicenter for the 1964 earthquake was in the Prince Williams Sound area (between Anchorage and Valdez) of south central Alaska, the aftershock area extended ~300 km to the east and ~800 km to the southwest (to southwest of Kodiak). Two areas of high slip in the 1964 event correspond to seismologically determined areas of high moment release: (1) the Prince William Sound asperity had an average slip of 18 m and (2) the "Kodiak asperity" had an average slip of 10 m [*Johnson et al.*, 1996; *Christensen and Beck*, 1994; *Holdahl and Sauber*, 1994]. In our discussion of the factors that contribute to ongoing crustal deformation across Kodiak we consider only the contribution of the Kodiak asperity. *Wells et al.* [2003] noted that areas of high coseismic slip commonly occurred beneath the prominent gravity lows outlining a deep-sea terrace low. The location of the Kodiak asperity does not seem to be associated with a prominent forearc basin gravity low.

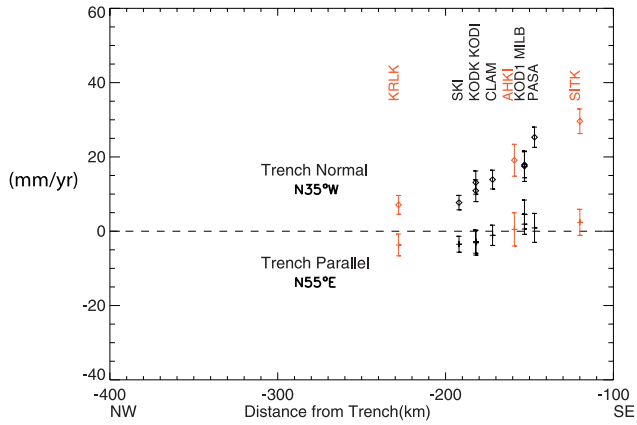

Figure 3. Station velocities resolved into trench-normal and trench-parallel components as a function of distance from the trench (taken to be from the southeastern most extent of the 4000 or 5800 m bathymetry contour). The error bars are two sigma. The station names are indicated along the top of the graph, the black data points are from northeastern Kodiak, and southwestern Kodiak stations are given in red. Positive velocities for the trench normal component indicate motion away from the trench (toward the volcanic arc on the Alaska Peninsula). Negative velocities for the trench parallel component indicate a southwest directed velocity (Table 3).

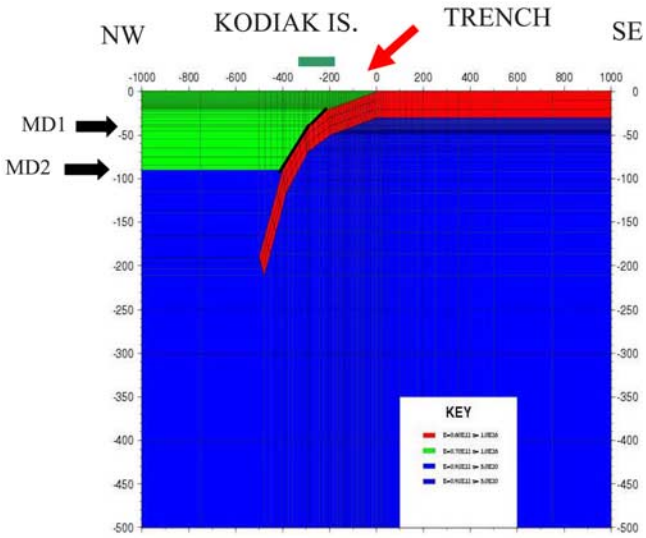

Figure 4. Two-dimensional finite element grid used in MD1 and MD2 models (modified from *Cohen* [1996], with the details of the model geometry given in Table 3 of Cohen). The "zero slab depth" location in our finite element and dislocation models is seaward (southeast) of the trench and corresponds to the projection of the slab to the surface. A low-viscosity zone occurs below a depth of 38 km in MD1 and below 90 km in the MD2 models (given in blue). In our reference model a viscosity of 1×10^{26} Pa s is assumed for the continental crust/mantle (green) and subducting plate (red), and a viscosity of 5×10^{19} Pa s is assumed for the low-viscosity region (blue). The dark line between the downgoing Pacific plate (in red) and the overriding continental plate (in green) represents the region of reduced slip during the 1964 earthquake and partial locking during the interseismic time interval in some models.

[20] In addition to the trench parallel variability in the coseismic slip in the 1964, changes in the coseismic slip and interseismic locking depth as a function of distance from the Aleutian Trench occur as well. In general, the seismogenic zone along the subduction plate interface is bounded by the upper and lower stability transition depths [e.g., *Scholz*, 1990]. The seaward updip limit is important for tsunami generation and the downdip limit is important for seismic hazard because it is used to infer the landward limit of the seismic source zone [e.g., *Oleskevich et al.*, 1999]. Since the boundary between the region of coseismic uplift and subsidence in the 1964 earthquake occurred on the Gulf of Alaska coastal portion of the island, earlier studies suggested that Kodiak is above the transition zone between interface slip in large earthquakes, postseismic creep, and aseismic creep at depth [*Ma et al.*, 1990; *Gilpin et al.*, 1994; *Gilpin*, 1995; *Stockman et al.*, 1997; *Savage et al.*, 1999; *Zweck et al.*, 2002]. These earlier Kodiak geodetic observations and modeling, however, hypothesize different downdip limits for coseismic slip and interseismic locking somewhere beneath Kodiak Island.

[21] We used aftershocks and tsunami studies of the 1964 earthquake, as well as thermomechanical models to give us an approximation of the updip and downdip limit of significant coseismic slip. Aftershocks following the 1964 earthquake suggest that significant coseismic slip started at approximately 100 km from the trench (toward northern Kodiak) [*Algermissen et al.*, 1969]. *Oleskevich et al.* [1999] estimated the 100–150°C temperature isotherm limit for clay dehydration between the Kenai Peninsula and Kodiak to be 80–160 km landward from the trench. Temperatures of 350–450°C are reached at depths of 80–100 km (close to the Alaska Peninsula); this region corresponds to the transition between brittle and ductile behavior for crustal rocks. The depth of the Moho in this region has been estimated to be 40–50 km. Near northeastern Kodiak there are few large earthquakes that have occurred near the trench over the last 20+ years (Figure 1). In contrast, near southwestern Kodiak, many moderate to large earthquakes have occurred between the trench and the Alaska Peninsula (Figure 1).

[22] The depth of the Aleutian trench ranges from about 4000 m near the northeastern part of the Kodiak to 5200 m a little farther to the southwest [*Beikman*, 1980]. The depth and curvature of the dipping slab in our finite element model (Figure 4) matches the dip of the upper slab surface inferred from background seismicity in the Kodiak region. However, the dip in our finite element model, near the trench, may be too steep. The dip of the shallow portion of the slab used in the finite element model is about as shallow as possible given the necessity to avoid an extreme aspect ratio of the elements that would create a numerical instability [*Cohen*, 1996].

[23] In addition to the megathrust fault (downgoing Pacific plate), Holocene surface faulting in and near the northeastern portion of the Kodiak has been mapped offshore on the Kodiak Shelf fault system [*Plafker et al.*, 1994] as well as within the Narrow Cape region [*Carver et al.*, 2002, 2003] near the station PASA (NC in Figure 2). The Border Ranges fault traverses onshore along the northwest coastline of the Kodiak (BR in Figure 2) but no clear evidence of Holocene slip on this fault system has been observed [*Gilpin*, 1995]. We assumed motion along the plate interface is the primary source of interseismic strain but we considered slip on the upper plate faults in our interpretation of horizontal velocities.

[24] The response of the Earth to tectonic loading depends on the rheological structure of the crust and upper mantle. The time-dependent response of the Earth has been shown to be important in Alaska for modeling geodetic data [*Brown et al.*, 1977; *Wahr and Wyss*, 1980; *Sauber et al.*, 1993; *Savage and Plafker*, 1991; *Cohen*, 1996; *Taylor et al.*, 1996; *Zheng et al.*, 1996; *Freymueller et al.*, 2000; *Sauber et al.*, 2000; *Zweck et al.*, 2000; *Freymueller et al.*, 2001]. Two time-dependent processes are particularly important in this region of large and great earthquakes. These are fault creep occurring downdip of the coseismic rupture plane and viscoelastic shear flow in the ductile portions of the lower crust and upper mantle (see summary by *Cohen* [1999]). Both of these mechanisms are stimulated by the coseismic transfer of stress from the shallow seismogenic portions of the Earth to greater depths. To evaluate interseismic and postseismic mechanisms that could account for our geodetic observations between 1993 and 2001, we calculated the predicted average surface displacement rate for alternate Earth models. We used

primarily a two-dimensional (2-D) plane strain finite element grid in TECTON [*Melosh and Raefsky*, 1981] for these calculations (Figure 4). The 2-D calculations of surface slip do not represent all features associated with heterogeneous coupling [*Dmowska et al.*, 1996]. The finite element grid across the plate boundary includes a shallow dipping subducting slab and both an oceanic crust-mantle and a continental crust-mantle (Figure 4). Because of our uncertain knowledge of the Earth's response to tectonic loading on the timescale of years, we explored alternate interface slip distributions and rheological models for the post-1964 coseismic and interseismic time periods. Because of the low viscosities in the lower crust and upper mantle ($\sim 10^{19-20}$ Pa s) inferred from most studies in Alaska, we assumed the current response of Kodiak to major late Pleistocene deglaciation and sea level rise to be insignificant. Recent glacial fluctuations on Kodiak are small and are not modeled as well.

[25] Simplifying the formulation given by *Cohen* [1999], we calculated the surface velocity over our time frame of interest due to the viscoelastic response to three major conceptual elements: (1) plate motion over the last 30+ years, (2) the 1964 earthquake, and (3) downdip creep below the region of maximum slip in the 1964 earthquake (Figure 4). The strain accumulation associated with plate motion was calculated as the viscoelastic response to back slip on the shallow portion of the plate interface. Although the viscoelastic response to coseismic slip in the 1964 earthquake is dependent on the (coseismic) slip distribution assumed as well as the viscosity structure, in general this effect is smaller than that due to plate motion, especially 30+ years after the earthquake. Creep on the plate interface can be time-dependent as well. Studies from the Prince William Sound area have suggested this is an important mechanism [*Brown et al.*, 1977; *Cohen*, 1996; *Cohen et al.*, 1995; *Freymueller et al.*, 2000; *Cohen and Freymueller*, 2001, 2004]. Although we explore a range of creep models, greater spatial and temporal resolution of surface velocities is needed to resolve the time-dependent changes in downdip creep.

4.1. Coseismic Slip in the 1964 Earthquake

[26] Numerous models of slip from the 1964 earthquake have been proposed and we will not attempt to summarize all the studies here. As mentioned earlier, the more recent models include a region of high slip referred to as the "Kodiak asperity" but studies differ in the location and magnitude of slip in this asperity [*Christensen and Beck*, 1994; *Holdahl and Sauber*, 1994; *Gilpin et al.*, 1994; *Gilpin*, 1995; *Johnson et al.*, 1996]. *Gilpin* [1995] included the most extensive Kodiak tide gauge and geologic data set and he inverted for slip across three different regions of Kodiak but not other regions (i.e., the Prince William Sound region that slipped in the 1964 earthquake). Gilpin's results also suggest that slip offshore extending to below northeastern Kodiak was larger than in southwestern Kodiak.

[27] The geologic and geodetic measurements used as constraints in the recent coseismic models actually bracket up to 14 months of slip. Thus estimates for "coseismic slip" include short-term postseismic processes such as fault slip in aftershocks, both on the plate interface and within the surrounding region, downdip creep, and any very short term anelastic response of the Earth. Also, it is important to note that for most of the coseismic slip models the vertical displacements (from offset of barnacles, tide gauge data, leveling) were the primary constraint. For more recent data used to estimate interseismic strain rates, such as our geodetic observations, the horizontal rate of deformation is the better constrained component.

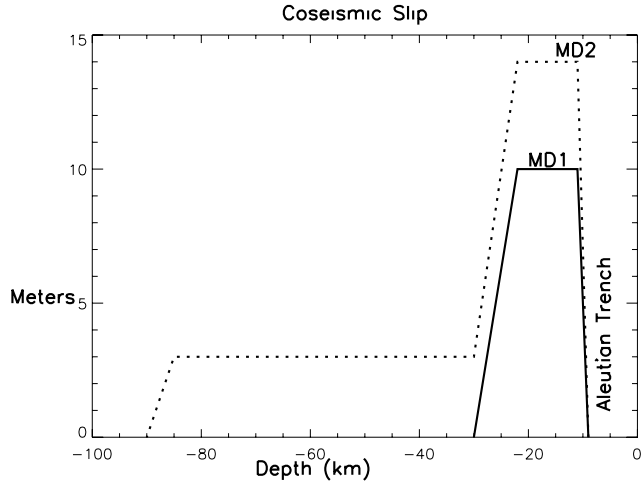

Figure 5. Coseismic slip (meters) in the 1964 earthquake as a function of depth for the MD1 (solid line) and MD2 (dashed line) models. The MD2 model includes reduced slip between 22 and 90.

[28] In this section we refine the coseismic slip models suggested by earlier studies to make our 2-D models specific to the two regions with geodetic observations. We used the tide gauge data summarized by *Gilpin* [1995] from their "northern" and "southern" Kodiak regions.

[29] For model 1 (MD1) we used a coseismic slip of 10 m for the depth range between 11 and 22 km (modified from *Holdahl and Sauber* [1994] and *Johnson et al.* [1996]). We assumed a linear transition to zero slip between 9 and 11 km and between 22 and 30 km (Figures 4 and 5, solid line without creep between 30 and 90 km). In such a model, slip in the 1964 earthquake was shallow and any postseismic response was associated with a fairly shallow (<40 km) low-viscosity zone.

[30] The second model MD2 is partially based on the maximum slip in northeastern Kodiak given by *Gilpin* [1995] (Figures 4 and 5); the coseismic slip is higher (MD1 above multiplied by 1.4 m) and we assumed short-term postseismic creep below the seismogenic zone (up to 3 m between depths of 22 and 90 km). In this model we assumed a deeper (>90 km) low-viscosity zone corresponding to temperatures >350°C. For southwestern Kodiak we multiplied both MD1 and MD2 models by 0.5 (half the coseismic slip as suggested by earlier studies). The 1964 coseismic subsidence and uplift values for the northwest (black, in Figure 6) and southeast (red) are clearly different.

[31] The predicted coseismic displacements due to these alternate coseismic slip distributions are compared in Figure 6. Although the two coseismic models would place different boundary conditions on the top of the

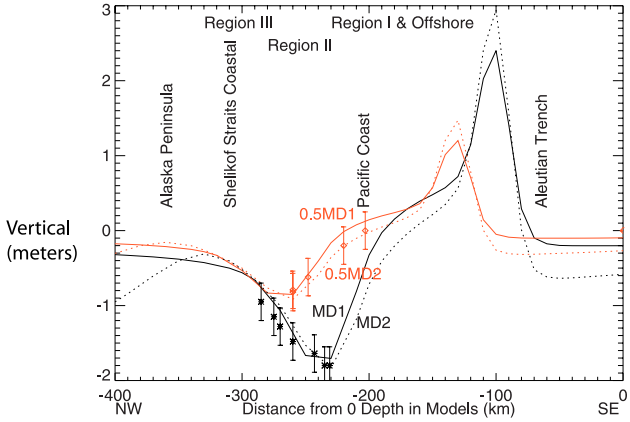

Figure 6. Predicted coseismic vertical displacement as a function of distance for the two slip models in Figure 5 along with coseismic data (asterisk with error bar for the north and diamond with error bar in red for the south) from *Plafker* [1969]. Model 1 (MD1) is given by a solid line and model 2 (MD2) is given by a dotted line, in black for northeastern Kodiak and in red for southwestern Kodiak. The coseismic data of *Plafker* [1969] given here correspond to a time interval of up to 14 months (see text). The downdip slip in MD2 between 22 and 90 km is assumed to represent a longer postseismic time interval.

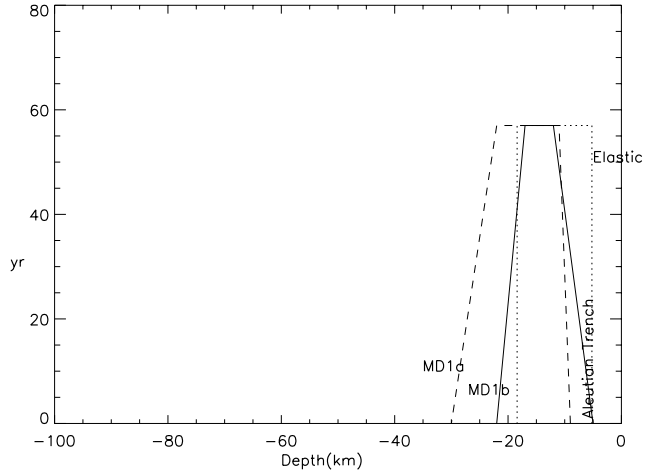

Figure 7. Input slip (mm/yr) for interseismic time period as a function of depth for elastic (dotted), MD1a (dashed), and MD1b (solid line).

asthenosphere right after an earthquake, the available vertical displacements at the surface cannot distinguish them.

4.2. Interseismic Model (1993–2001)

[32] As discussed above, a number of mechanisms could influence the surface deformation rates obtained in this study, ~30–40 years following the 1964 earthquake. There are numerous studies of the postseismic response to the 1964 earthquake especially in the Kenai region (see summary of *Cohen and Freymueller* [2004]). Additionally, in the Kodiak region, *Gilpin et al.* [1994] and *Gilpin* [1995] used permanent and temporary tide gauge data from the islands to estimate a downdip, postseismic creep of ~3 m during the 25 years following the earthquake. This is about the amount of creep inferred for the Kenai region over a similar time period [*Cohen et al.*, 1995; *Freymueller et al.*, 2000]. On the basis of their analysis of tide gauge data, *Savage and Plafker* [1991] postulated that in addition to downdip creep, a slower viscoelastic relaxation of the low-viscosity mantle could be important over a longer timescale. We included the viscoelastic response to 1964 slip in both end member models, albeit at different depths.

4.2.1. Elastic Dislocation Model

[33] Locking of the plate interface at shallow depths is assumed to exert the greatest influence on the interseismic rate of deformation over 30 years after the 1964 earthquake. For a point of reference we present the elastic dislocation model used by *Savage et al.* [1999] to represent back slip at the relative plate rate on a shallow main thrust zone. *Savage et al.* [1999] used a nonlinear inversion program to determine the parameters for a dislocation model which best fits their southeastern Kodiak data. They assumed a dip of 5° along the locked plate interface. The locked zone width of 152 km (57 km to 209 km downdip, Figure 3 [*Savage et al.*, 1999]) and a back-slip rate of 57 mm/yr were estimated. Their locked zone was between depths of 5 and 18 km (Figure 7).

[34] The elastic slip model is shown Figure 7, and the comparison to data is shown in Figures 8 and 9. If the elastic profile is shifted relative to the trench (the assumed zero depth is farther southeast due to, for instance, a shallower dip) the elastic model will fit the horizontal data better near the locked main thrust zone. The elastic model however does not account for horizontal data farther inland. The predicted trench normal rate of deformation from northeastern and southwestern Kodiak shown in Figure 8 illustrates the important contribution the shallow locked zone makes to ongoing strain accumulation but the data/

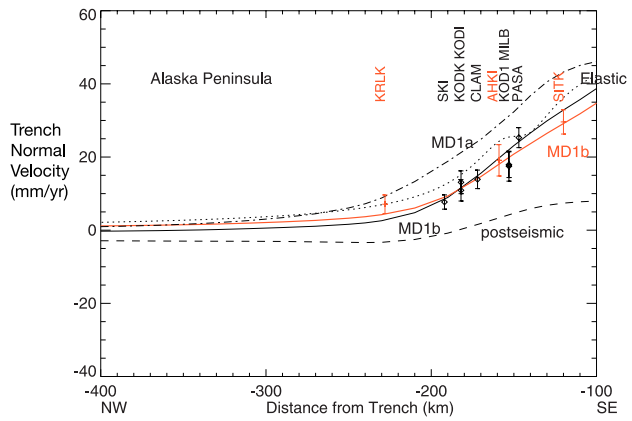

Figure 8. Comparison of the geodetically estimated rate of deformation (trench normal) to the predicted horizontal velocity from the elastic (dotted, *Savage et al.* [1999]) and the MD1a (solid), MD1a (solid red for southwestern Kodiak), and MD1b (dashed) viscoelastic models. Northeastern Kodiak trench-normal data are given in black, and the southwestern Kodiak data are given in red. Note that none of these models predict trench directed velocities at distances of ~300–400 km (Alaska Peninsula).

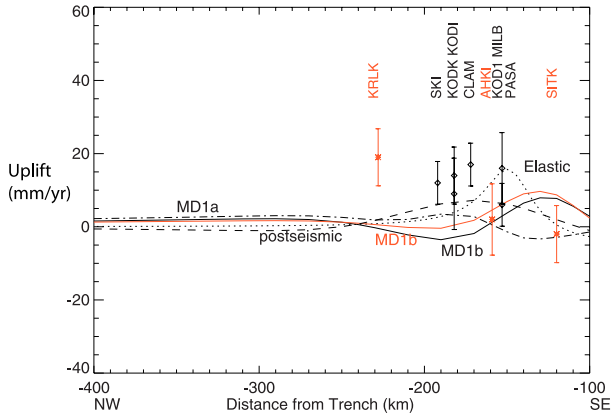

Figure 9. Comparison of geodetically estimated vertical displacement rate to the predicted vertical velocity from the elastic (dotted, *Savage et al.* [1999]) and the MD1a (solid), MD1a (solid red for southwestern Kodiak), and MD1b (dashed) viscoelastic models. The vertical uplift rate at KRLK is not matched by any of the models.

model discrepancy also suggests that other processes could contribute.

4.2.2. Predicted Time-Dependent Surface Displacement Rate

[35] In the MD1 interseismic models, the transient component of surface deformation is primarily due to the time-dependent viscous relaxation of a shallow (>38 km) low-viscosity zone instead of time-dependent, downdip creep. In MD1 we assumed that most of the upper crust (elastic layer) ruptured during the 1964 earthquake (Figure 7, dashed line). For our reference model given in the figures we assumed a viscosity of η of 5×10^{19} Pa s and rigidity (G) of 0.6×10^{19} Pa. This corresponds to a Maxwell time, τ, of ~26 years, where $\tau = \eta/G$. The influence of the assumed viscosity η is discussed later. In general postseismic relaxation of the 1964 displacement would cause subsidence and arc directed horizontal motion above the 1964 rupture, near the Gulf Alaska coastal region of Kodiak (Figure 8). Inland of the maximum 1964 coseismic subsidence (toward the Alaska Peninsula), postseismic relaxation would cause trench directed motion.

[36] In MD1a we used the coseismic region as a proxy for the region that is locked during the interseismic time period. Specifically, between 11 and 22 km we imposed 57 mm/yr of back slip and between 9 and 11 km and 22 and 30 km, the imposed plate rate of back slip was reduced to zero. For model MD1b, we used a shorter locked zone that is closer in extent to the elastic model of Savage (Figure 7, solid line).

[37] In Figures 8 and 9, we compared the predicted horizontal and vertical displacement rates for MD1a,b to the horizontal and vertical data and the elastic model. The MD1a,b and the elastic model predictions are similar to the observed horizontal data near the locked main thrust zone. Farther inland, however, but trench-directed motion on the Alaska Peninsula is not predicted (1993–2001, http://quake.wr.usgs.gov/research/deformation/gps/auto/KatmaiKodiak).

[38] In the MD2 suite of models the low-viscosity layer is deeper (≥90 km) and postseismic creep from the base of the seismogenic zone down to 90 km is included and evaluated (Figures 4 and 10 and Tables 4 and 5). In MD2a, b (Table 4) we assumed that the region of high coseismic slip was also the region that was locked during the interseismic time period (i.e., the MD2 coseismic model). In contrast, for MD2c,d, we assumed the region of full interseismic coupling was slightly smaller than the region of high coseismic slip in the 1964 earthquake; that is, closer to the locked region of *Savage et al.* [1999] but the MD2c,d viscoelastic model includes downdip creep as well.

[39] We calculated the response to 10–60 mm/yr of creep between the downdip extent of the locked zone to 90 km. A model with little (MD2a) or no creep between 30 and 90 km predicts a higher horizontal rate of deformation (arc directed) than observed in northeastern Kodiak (Figure 11). At the other extreme, a model (not shown) that includes 60 mm/yr of creep under predicts the horizontal rate of deformation directed arcward.

[40] Since the amount of coseismic slip is different between northeastern and southwestern Kodiak, we included the region-specific postseismic relaxation due to coseismic slip for the calculations; thus the postseismic viscous relaxation is hypothesized to be smaller in southwestern Kodiak. Additionally we hypothesize that the magnitude of creep scales as a function of coseismic slip as well. MD2c in red represents the predicted horizontal rates for southwestern Kodiak (Figure 11). The vertical data are best predicted by the MD2a,b models with the wider locked main thrust zone (Figure 12).

[41] The model that best predicts the horizontal data, especially near the trench, is MD2c. To interpret the relative importance of the various mechanisms that contribute to this model, we plotted the individual contribution from each of the deformation mechanisms as well (Figure 13).

[42] Each of these models predicts different horizontal velocities for the Alaska Peninsula region (Figure 11) as well. The stations from the Alaska Peninsula in the Katmai volcano region have small, horizontal velocities (3–4 mm/yr) that are primarily trench directed in a North America fixed reference frame (1993–2001, http://quake.wr.usgs.gov/

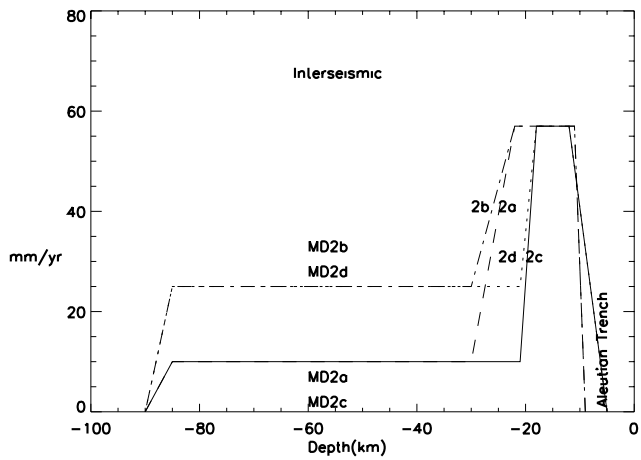

Figure 10. Input slip (mm/yr) for interseismic time period as a function of depth for MD2a (dashed + solid), MD2b (dot-dotted), MD2c (solid), and MD2d (dot-dash-dotted).

Table 4. Interseismic Model Parameters

Model	Coseismic Model	Depth of Low Viscosity, km	Interseismic Locked Zone	Creep Region Rate, mm/yr
Elastic	none	none	$5 \leq$ z km ≤ 18	none
MD1a	$9-11 \leq$ z km $\leq 22-30$	38	$9-11 \leq$ z km $\leq 22-30$	none
MD1b	$9-11 \leq$ z km $\leq 22-30$	38	$5-12 \leq$ z km $\leq 17-22$	none
MD2a	dotted line in Figure 4b	90	dash plus solid in Figure 4d	10
MD2b	dotted line in Figure 4b	90	dash-dotted in Figure 4d	25
MD2c	dotted line in Figure 4b	90	solid line in Figure 4d	10
MD2d	dotted line in Figure 4b	90	dot and dash-dotted in Figure 4d	25

research/deformation/gps/auto/KatmaiKodiak). These results are similar to that observed in the Kenai Peninsula, which have been attributed to dip-slip creep on a portion of the plate interface below the locked main thrust zone [*Freymueller et al.*, 2000]. The higher creep models (MD2b,d) however, over predict the amount of trench directed motion on the Alaska Peninsula. Future measurements on the Alaska Peninsula and along the western coast of Kodiak as part of the EarthScope plate boundary observatory (PBO) network will provide more robust constraints on deep slip mechanisms.

4.2.3. Variable Viscosity Values and the Preferred Model

[43] The postseismic component is generally small relative to interseismic strain and creep but we explored various viscosity values to test the uniqueness of the viscosity used to calculate the postseismic response to the 1964 earthquake (Figure 14). We varied the lower crust/upper mantle vis-

Table 5. Event Locations, Fault Plane Parameters, and Date

Event	Longitude, °E	Latitude, °N	Depth, km	Str1	Dip1	Rake1	Str2	Dip2	Rake2	Date, mmddyr
1	−154.43	58.09	134	42	65	22	302	70	153	112777
2	−151.21	56.30	15	265	8	119	55	83	86	071978
3	−154.16	56.20	34	244	13	94	60	77	89	070680
4	−151.38	56.91	19	215	9	78	47	82	92	090682
5	−155.43	56.95	68	85	59	−18	185	75	−147	112683
6	−154.18	58.62	119	334	25	−164	229	83	−65	032384
7	−154.06	58.58	106	319	50	168	56	81	41	102785
8	−153.38	56.11	23	220	18	75	56	73	95	030686
9	−153.20	58.88	88	89	64	12	353	80	153	052386
10	−153.21	56.06	15	241	11	105	46	79	87	091686
11	−152.28	56.30	33	228	8	85	53	82	91	052087
12	−154.64	57.70	73	319	28	−176	225	88	−62	061689
13	−153.17	58.30	60	176	62	−154	73	67	−31	030890
14	−153.09	56.89	15	212	9	61	62	82	94	052990
15	−155.48	56.34	65	0	70	173	93	84	20	080192
16	−154.87	57.24	67	358	29	−148	239	75	−65	091292
17	−153.81	56.80	27	61	33	−67	214	60	−105	042293
18	−149.96	58.49	32	141	23	−150	23	79	−70	121594
19	−152.83	57.03	15	58	4	−66	214	87	−91	030396
20	−151.54	56.14	33	218	20	60	70	72	101	120896
21	−152.07	56.73	33	299	5	159	50	88	85	110898
22	−152.86	56.48	15	209	11	101	18	79	88	050699
23	−152.58	56.21	19	225	9	74	61	81	93	050799
24	−154.78	58.15	89	64	49	−17	165	78	−138	082699
25	−154.35	57.35	54	357	63	−180	267	90	−27	120699
26	−154.38	57.22	48	350	37	−161	245	79	−55	120799
27	−154.04	57.24	66	5	75	178	96	88	15	011600
28	−149.29	57.47	15	302	55	136	61	55	45	012300
29	−154.44	57.41	43	350	10	−139	219	84	−83	030800
30	−154.28	57.48	53	26	15	−96	212	75	−88	050800
31	−152.84	58.97	91	330	56	−174	236	85	−35	051900
32	−150.18	58.65	36	82	63	24	341	69	150	062800
33	−154.22	57.54	52	356	47	−161	253	76	−44	071100
34	−154.24	57.58	43	224	42	−36	341	67	−127	091900
35	−153.70	58.00	41	98	60	35	349	60	145	092500
36	−153.56	56.99	21	224	8	74	60	82	92	011001
37	−153.63	56.51	25	225	7	92	43	83	90	021101
38	−150.99	57.06	30	332	66	170	66	81	24	071901
39	−154.97	58.82	147	63	64	26	321	67	151	072801
40	−155.11	57.63	122	278	35	73	119	57	102	082901
41	−151.26	58.50	19	218	32	−31	335	74	−118	090502
42	−151.44	58.33	12	154	8	−14	258	88	−98	012004

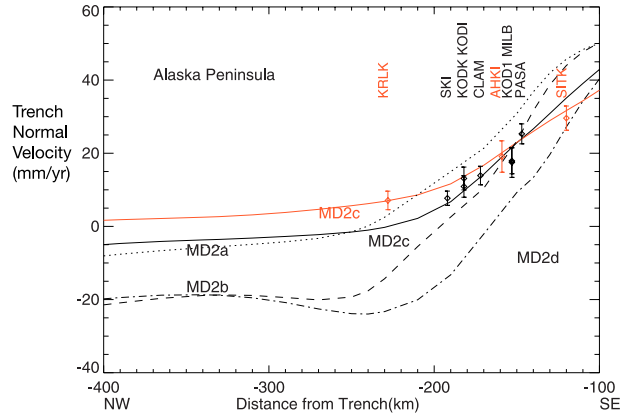

Figure 11. Comparison of the predicted horizontal velocities for the four MD2 models of Table 4, plus southwestern Kodiak for the preferred model of MD2c (red), to the observed horizontal velocities.

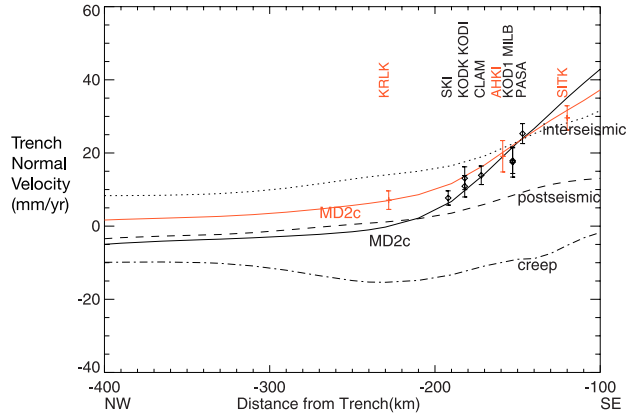

Figure 13. Observed versus predicted horizontal velocities for the MD2c model including the individual elements (dotted, interseismic; dashed, postseismic; and dash-dotted, creep) and all three components together (total, solid line). Data description is as given in Figure 8.

cosity between 10^{19} and 5×10^{20} Pa s. With a viscosity of 10^{19} Pa s the Maxwell time, τ, is just 5 years and for 5×10^{20} Pa s, τ = 264 years. The models with the viscosity values of 10^{19} and 5×10^{20} Pa s do not approximate the northeastern Kodiak data. The 10^{20} Pa s model approximates the general drop off in velocity but underpredicts the rate as a function of distance from the trench.

5. Discussion

5.1. Sources of Time-Dependent Deformation

[44] On the basis of our modeling of the geodetic observations, time-dependent creep and possibly postseismic viscoelastic relaxation may be a significant source of the measured surface velocities. Because of the large uncertainties in our short-term vertical results, we evaluated this conjecture by examining other data from the region of the 1964 earthquake. Long-term and temporary tide gauge measurements have been used as well to estimate uplift rates since the 1964 earthquake [*Savage and Plafker*, 1991; *Gilpin*, 1995; *Cohen and Freymueller*, 2001]. Temporary tide gauge measurements have been used to constrain coseismic slip in the 1964 earthquake and additionally these measurements were made between 1965 and 1993 on Kodiak, primarily to the northwest Kodiak GPS stations [*Gilpin et al.*, 1994; *Gilpin*, 1965]. The 1964–1993 vertical measurements show less scatter, as a function of distance from the trench, than our short-term vertical rates.

[45] In Figures 15 and 16 we compared the tide gauge uplift values (1965–1993) to the predicted uplift assuming the model parameters given by the elastic and MD1a,b and MD2b,c models. The rate of uplift for the elastic model is much higher than the observed uplift rates for 1965–1993 and the MD1a,b (interseismic strain plus postseismic relaxation) models predict a lower rate of uplift than is observed (Figure 15). For this earlier time period, the total uplift is better predicted by the model with the higher creep rate of 25 mm/yr (MD2b, Figure 16).

[46] Other studies have suggested a time variable uplift rate due to downdip creep as well. On the basis of the tide gauge data from Woman's Bay (<1 km from KODK, KODI and the old VLBI mark), *Cohen and Freymueller* [2001]

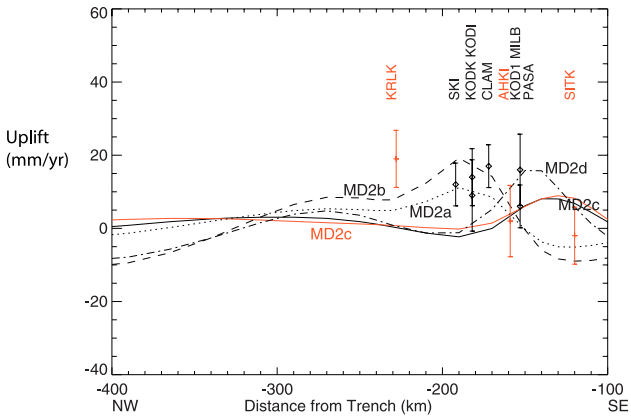

Figure 12. Observed versus vertical displacement rate for the four MD2 models plus southwestern Kodiak model of MD2c.

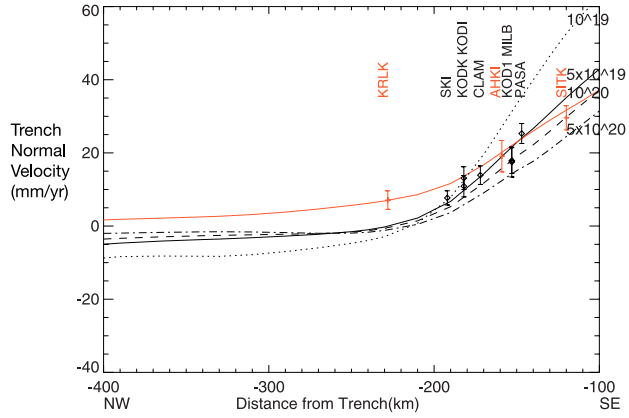

Figure 14. Predicted horizontal velocity for the MD2c model assuming four different viscosities 10^{19}, 5×10^{19}, 10^{20}, and 5×10^{20} Pa s and for southwestern Kodiak MD2c (solid red) for a viscosity of 5×10^{19} Pa s.

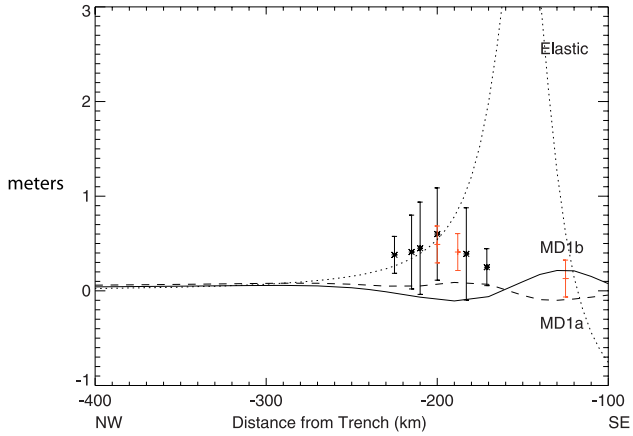

Figure 15. Temporary tide gauge data of *Gilpin* [1995] (asterisk plus error bar) compared to the predicted vertical displacement between 1965 and 1993 assuming the model parameters over a 28 year time period for elastic, MD1a, and MD1b. Note that the maximum uplift predicted for the elastic model was 4.2 m.

estimated an average uplift rate of 14 ± 1 mm/yr between 1967 and 1998, but they suggest there is a significant decrease in the uplift rate as a function of time. They estimated an uplift rate of 15 mm/yr for 1985 and 8 mm/yr for 1995.

[47] Recent earthquakes (southwestern Kodiak 1999–2001, see discussion in section 1) and possibly creep have occurred below the region of high coseismic slip in the 1964 earthquake in the last decade. Around the same time as the earthquakes in southwestern Kodiak, an aseismic slip event occurred (1998–2001) in the Anchorage region [*Freymueller et al.*, 2001]. *Freymueller et al.* [2001] hypothesized that the southeast directed surface displacement was due to creep on a segment of the plate interface downdip from the locked main thrust zone. The creep that occurred in the region downdip of the 1964 coseismic slip was of longer duration, and possibly over a spatially larger region, than the North Cascadia episodic tremor and slip events [*Dragert et al.*, 2004]. Instead this slip event may have been more the like the Guerrero aseismic slip event that started in October 2001 and lasted 6–7 months over an area of 550 km x 250 km [*Kostoglodov et al.*, 2003]. The slip events below the seismogenic zone generally increase the stress on the locked shallow portion of the main thrust zone and at times may lead to large earthquakes [*Ozawa et al.*, 2002; *Kostoglodov et al.*, 2003; *Dragert et al.*, 2004].

5.2. Long-Term Vertical Uplift Rates Compared to Our Geodetic Uplift Rates

[48] Kodiak is located near the northern extent of the Shuttle Radar Topography Mission (SRTM) orbit. Multiple C-band swaths were processed into a digital elevation model (DEM) by the Jet Propulsion Laboratory (see http://www.jpl.nasa.gov/srtm and *Farr and Kobrick* [2001]). Landsat 7 images and a SRTM-derived DEM were used by *Carver et al.* [2003] to identify a coastal marine terrace across the northeastern and northern portion of Kodiak. The terrace includes broad planar surfaces up to several kilometers wide that border the modern coast line. The terrace increases in elevation uniformly from about 15 m on the northwest region of Kodiak to about 40 m in the central region of the island (near the city of Kodiak, Figure 2). On the basis of the assumption that the surface had been cut by shoreline planation during the last interglacial (probably an oxygen isotope stage 5e, 120–130 ka), *Carver et al.* [2003] estimated an average uplift rate of 0.15 mm/yr for the northwest coast region to 0.3 mm/yr for central Kodiak (Figure 1). The uplift estimated from the terrace data suggests that within the transition region of the 1964 coseismic uplift and subsidence (northeast coastal region of Figures 1 and 2) the highest rate of long-term uplift is associated with crustal shortening on upper crustal faults. For instance, at Narrow Cape on Kodiak's northeast coast, the elevation of the terrace is about 80 m and it is 100 m on nearby Ugak Island (Figure 2). Mapping and trench studies of several lineaments identified from Landsat 7 and SRTM data show evidence for late Pleistocene and Holocene surface fault rupture in the vicinity of the Kodiak launch facility at Narrow Cape [*Carver et al.*, 2003]. In contrast, the highest rate of short term (geodetic uplift) is farther inland. However, the region of short-term uplift corresponds to the region of maximum subsidence in the 1964 earthquake.

6. Summary

[49] The new geodetic results reported in this study from northeastern Kodiak document the change in deformation rates across a transition region between uplift and subsidence in the 1964 earthquake. Earlier VLBI results indicate that a simple elastic dislocation model used to represent interseismic strain accumulation was inadequate to account for the observed horizontal and vertical rates as a function of distance from the trench [*Ma et al.*, 1990]. Later studies further indicate the importance of time-dependent uplift rates following the 1964 earthquake [e.g., *Cohen and Freymueller*, 2001]. Additional permanent GPS stations across Kodiak and on the Alaska Peninsula could provide important constraints on downdip, time-dependent processes.

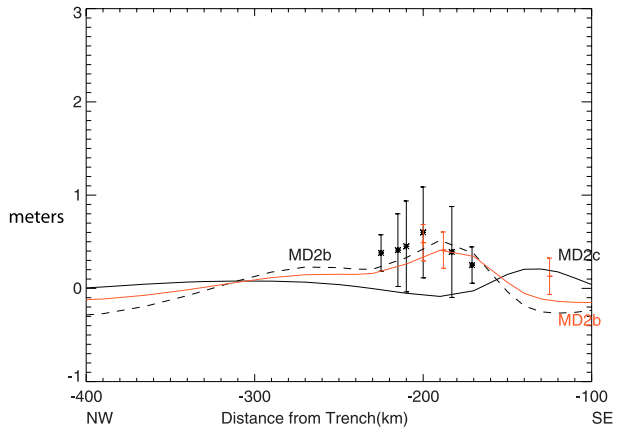

Figure 16. Temporary tide gauge data of *Gilpin* [1995] (asterisk plus error bar) compared to the predicted vertical displacement between 1965 and 1993 assuming the model parameters over a 28 year time period for MD2b (dashed line), MD2c (solid line), and MD2c (solid red). The higher creep rate model of MD2b better matches the earlier uplift rate observed from 1965 to 1993.

In this study, we suggest that the recent horizontal (trench perpendicular component) and earlier vertical uplift data across Kodiak can be accounted for back slip representing a locked main thrust zone, downdip creep, and coseismic slip in the 1964 earthquake if the viscoelastic response to each is included. Northeastern and southwestern Kodiak have different interface slip histories and interseismic strain predictions. A change in the orientation of the horizontal velocity vectors occurs above the downdip segment of the locked main thrust zone. We hypothesize that the horizontal, trench-parallel component of slip will be released as left-lateral slip on trench parallel, upper plate faults which would result in southwest translation of western Kodiak.

[50] **Acknowledgments.** Early work on establishing the northeastern Kodiak Island geodetic stations and the construction of the KODK station were greatly facilitated by the late Mark Bryant (who died on 14 January 2002 at the age of 41), Robert LeMoine, and Thomas Clark. The GSFC Alaska team misses Mark's technical expertise, personal integrity, and gracious, southern style, and we dedicate this paper to his memory. Eric Linscheid of the Kodiak Island High School has participated in many aspects of this study and most recently has been downloading the KODK station. Robert LeMoine's expert surveying assistance over several summers was greatly appreciated. The U.S. Coast Guard graciously allowed us to locate the KODK monument and receiver at Kodiak Island base. Roy Ecklund put in the geodetic marks for CLAM, SKI0, and PASA. Nino Fiorentino, Steve Nerem, Steve Fisher, Claudia Carabajal, and Jim Long contributed their field expertise to at least one observation campaign between 1993 and 2001. We thank the numerous students of Kodiak Island High School for their participation in the GPS observation campaigns in 1995, 1997, and 1999; Yehuda Bock and Paul Jamason at SOPAC, Scripps Institute of Oceanography, for helping us set up KODK as an IGS station; and Simon McClusky and Tom Herring for GAMIT/GLOBK assistance. Karen Wendt (USGS) kindly helped us acquire the Katmai (1993–1997) GPS data. Constructive suggestions by reviewers Jeff Freymueller and Jim Savage are greatly appreciated. The numerical calculations reported here were generated using a modified version of the finite element code TECTON developed by H. Jay Melosh. We especially thank the JPL SRTM team for providing the SRTM data used in various aspects of this study. This research was supported by NASA's Solid Earth and Natural Hazards program, SRTM investigation (921-622-74-10-04), the earlier NASA Dynamics of the Solid Earth DOSE program, and the NASA Goddard Space Flight Center's Director's Discretionary Fund.

References

Algermissen, S. T., W. A. Rinehart, R. W. Sherburne, and W. Dillinger (1969), Preshocks and aftershocks of the Prince William Sound earthquake of March 28, 1964, *Coast Geod. Surv. Publ., 10-3*, vol. II, parts B and C.

Becker, T., and A. Braun (1998), New program maps geoscience data sets interactively, *Eos Trans. AGU*, *79*, 505, 508.

Beikman, H. M. (1980), Geologic map of Alaska, special map, scale 1:2,500,000, 2 sheets, U.S. Geol. Surv., Reston, Va.

Bock, Y., J. Behr, P. Fang, J. Dean, and R. Leigh (1997), Scripps Orbit and Permanent Array Center (SOPAC) and Southern California Permanent Array Center (PGGA), in *The Global Positioning System for the Geosciences*, pp. 55–61, Natl. Acad. Press, Washington, D. C.

Brown, L. D., R. E. Reilinger, S. R. Holdahl, and E. I. Balazs (1977), Postseismic crustal uplift near Anchorage, Alaska, *J. Geophys. Res.*, *82*, 3369–3378.

Carver, G. A., R. A. Knecht, R. S. Davis, P. Saltonstall, and J. Sauber (2002), Holocene sea level changes and resettlement of maritime people in the eastern Aleutian and Kodiak Islands, Alaska, *Eos Trans. AGU*, *81*(48), Fall Meet. Suppl., Abstract U61A-04.

Carver, G. A., J. Sauber, W. R. Lettis, and R. C. Witter (2003), Use of SRTM and Landsat-7 data to evaluate seismic hazards, Kodiak Island, Alaska, paper presented at EGS-AGU-EUG Joint Meeting, Nice, France.

Christensen, D., and S. Beck (1994), The 1964 Prince William Sound earthquake: Rupture process and plate segmentation, *Pure Appl. Geophys.*, *142*, 29–53.

Cohen, S. C. (1996), Time-dependent uplift of the Kenai Peninsula and adjacent regions of south central Alaska since the 1964 Prince William Sound earthquake, *J. Geophys. Res.*, *101*, 8595–8604.

Cohen, S. C. (1999), Numerical models of crustal deformation in seismic zones, *Adv. Geophys.*, *41*, 133–233.

Cohen, S. C., and J. T. Freymueller (2001), Crustal uplift in the south central Alaska subduction zone: New analysis and interpretation of tide gauge observations, *J. Geophys. Res.*, *106*, 11,259–11,270.

Cohen, S. C., and J. T. Freymueller (2004), Crustal deformation in the southcentral Alaska subduction zone, *Adv. Geophys.*, *47*, 1–58.

Cohen, S. C., S. Holdahl, D. Captrette, S. Hilla, R. Safford, and D. Schutz (1995), Uplift of the Kenai Peninsula, Alaska, since the 1964 Prince William Sound earthquake, *J. Geophys. Res.*, *100*, 2031–2038.

Davies, J., L. Sykes, L. House, and K. Jacob (1981), Shumagin seismic gap, Alaska Peninsula: History of great earthquakes, tectonic setting, and evidence for high seismic potential, *J. Geophys. Res.*, *86*, 3821–3855.

DeMets, C., and T. H. Dixon (1999), New kinematic models for Pacific-North American motion from 3 Ma to present, I: Evidence for steady motion and biases in the NUVEL-1A model, *Geophys. Res. Lett.*, *26*, 1921–1924.

DeMets, C., R. G. Gordon, D. Argus, and S. Stein (1994), Effect of recent revisions to the geomagnetic reversal time scale on estimates of current plate motions, *Geophys. Res. Lett.*, *21*, 2191–2194.

Dmowska, R., G. Zheng, and J. R. Rice (1996), Seismicity and deformation at convergent margins due to heterogeneous coupling, *J. Geophys. Res.*, *101*, 3015–3029.

Doser, D. I., W. A. Brown, and M. Velasquez (2002), Seismicity of the Kodiak Island region (1964–2001) and its relation to the 1964 great Alaska earthquake, *Bull. Seism. Soc. Am.*, *92*, 3269–3292.

Dragert, H., K. Wang, and G. Rogers (2004), Geodetic and seismic signatures of episodic tremor and slip in the northern Cascadia subduction zone, *Earth Planets Space*, *56*, 1143–1150.

Dziewonski, A. M., and J. H. Woodhouse (1983), Studies of the seismic source using normal-mode theory, in *Earthquakes: Observation, Theory, and Interpretation*, edited by H. Kanamori and E. Boschi, *Proc. Int. Sch. Phys. Enrico Fermi*, *85*, 45–137.

Ekström, G. (1994), Rapid earthquake analysis utilizes the internet, *Comput. Phys.*, *8*, 632–638.

Farr, T., and M. Kobrick (2001), The Shuttle Radar Topography Mission, *Eos Trans. AGU*, *82*(47), Fall Meet. Suppl., Abstract G22B-0214.

Freymueller, J. T., and J. Beavan (1999), Absence of strain accumulation in the western Shumagin segment of the Alaska subduction zone, *Geophys. Res. Lett.*, *26*, 3233–3236.

Freymueller, J., S. C. Cohen, and H. J. Fletcher (2000), Spatial variations in present-day deformation, Kenai Peninsula, Alaska, and their implications, *J. Geophys. Res.*, *105*, 8079–8101.

Freymueller, J., C. Zweck, H. Fletcher, S. Hreinsdottir, S. C. Cohen, and M. Wyss (2001), The great Alaska "earthquake" of 1998–2001, *Eos Trans. AGU*, *82*(47), Fall Meeting Suppl., Abstract G22D-11.

Gilpin, L. M. (1995), Holocene paleoseismicity and coastal tectonics of the Kodiak Islands, Alaska, Ph.D. thesis, 357 pp., Univ. of Calif., Santa Cruz.

Gilpin, L. M., G. A. Carver, S. Ward, and R. S. Anderson (1994), Tidal benchmark readings and postseismic rebound of the Kodiak Islands, SW extent of the 1964 great Alaskan earthquake rupture zone, *Seismol. Res. Lett.*, *65*(1), 68.

Hansen, R. A., and N. A. Ratchkovski (2001), The Kodiak Island, Alaska, M_w 7 earthquake of December 6, 1999, *Seismol. Res. Lett.*, *72*, 22–32.

Herring, T. A. (2003), GLOBK, Global Kalman filter VLBI and GPS analysis program, Release 10.0, 98 pp., Mass. Inst. of Technol., Cambridge.

Holdahl, S., and J. Sauber (1994), Coseismic slip in the 1964 Prince William Sound earthquake: A new geodetic inversion, *Pure Appl. Geophys.*, *142*(1), 55–82.

Johnson, J. M., K. Satake, S. R. Holdahl, and J. Sauber (1996), The 1964 Prince William Sound earthquake, joint inversion of tsunami and geodetic data, *J. Geophys. Res.*, *101*, 523–532.

King, R. W., and Y. Bock (2003), Documentation for the GAMIT GPS analysis software: GAMIT, version 10.1, Mass. Inst. of Technol., Cambridge.

Kostoglodov, V., S. K. Singh, J. A. Santiago, S. I. Franco, K. Larson, A. Lowry, and R. Bilham (2003), A large silent earthquake in the Guerrero seismic gap, Mexico, *Geophys. Res. Lett.*, *30*(15), 1807, doi:10.1029/2003GL017219.

Ma, C., J. M. Sauber, L. J. Bell, T. A. Clark, D. Gordon, W. E. Himwich, and J. W. Ryan (1990), Measurement of horizontal motions in Alaska using very long baseline interferometry, *J. Geophys. Res.*, *95*, 21,991–22,011.

Mann, D., and J. Freymueller (2003), Volcanic and tectonic deformation on Unimak Island in the Aleutian Arc, Alaska, *J. Geophys. Res.*, *108*(B2), 2108, doi:10.1029/2002JB001925.

McCaffrey, R., P. C. Zwick, Y. Bock, L. Prawirodirdjo, J. F. Genrich, C. W. Stevens, S. S. O. Puntodewo, and C. Subarya (2000), Strain partitioning during oblique plate convergence in northern Sumatra: Geodetic and

seismologic constraints and numerical modeling, *J. Geophys. Res.*, *105*, 28,363–28,376.
McClusky, S., et al. (2000), Global Positioning System constraints on plate kinematics and dynamics in the eastern Mediterranean and Caucasus, *J. Geophys. Res.*, *105*, 5695–5719.
Melosh, H. J., and A. Raefsky (1981), A simple and efficient method for introducing faults into finite element computations, *Bull. Seismol. Soc. Am.*, *71*, 1391–1400.
Nishenko, S. P., and K. H. Jacob (1990), Seismic potential of the Queen Charlotte-Alaska-Aleutian seismic zone, *J. Geophys. Res.*, *95*, 2511–2532.
Oleskevich, D. A., R. D. Hyndman, and K. Wang (1999), The updip and downdip limits to great subduction earthquakes: Thermal and structural models of Cascadia, south Alaska, SW Japan, and Chile, *J. Geophys. Res.*, *104*, 14,965–14,991.
Ozawa, S., M. Murakami, M. Kaidzu, T. Tada, T. Sagiya, Y. Hatanaka, H. Yarai, and T. Nishimura (2002), Detection and monitoring of ongoing aseismic slip in the Tokai region, central Japan, *Science*, *298*, 1009–1012.
Plafker, G. (1969), Tectonics of the March 27, 1964, Alaska earthquake, *U.S. Geol. Surv. Prof. Pap.*, *543-I*, 74 pp.
Plafker, G., J. C. Moore, and G. R. Winkler (1994), Geology of the southern Alaska margin, in *The Geology of North America*, vol. G-1, *The Geology of Alaska*, edited by G. Plafker and H. C. Berg, pp. 389–450, Geol. Soc. of Am., Boulder, Colo.
Pulpan, H., and C. Frohlich (1985), Geometry of the subducted plate near Kodiak Island and lower Cook Inlet, Alaska determined from relocated earthquake hypocenters, *Bull. Seismol. Soc. Am.*, *75*, 791–810.
Ratchkovski, N. A., and R. A. Hansen (2001), Sequence of strong intraplate earthquakes in the Kodiak Island region, Alaska, 1999–2001, *Geophys. Res. Lett.*, *28*, 3729–3732.
Ryan, J. W., C. Ma, and D. S. Caprette (1993), NASA space geodesy program, GSFC data analysis: 1992, *NASA Tech. Memo, TM-104572*.
Sauber, J., T. A. Clark, L. J. Bell, M. Lisowski, C. Ma, and D. S. Caprette (1993), Geodetic measurement of static displacement associated with the 1987–1988 Gulf of Alaska earthquakes, in *Contributions of Space Geodesy to Geodynamics: Crustal Dynamics*, *Geodyn. Ser.*, vol. 23, edited by D. E. Smith and D. L. Turcotte, pp. 233–248, AGU, Washington, D. C.
Sauber, J., S. McClusky, and R. King (1997), Relation of ongoing deformation rates to the subduction zone process in southern Alaska, *Geophys. Res. Lett.*, *24*, 2853–2856.
Sauber, J., S. Stockman, and T. Clark (1998), Educational outreach strategy involves K-12 students in earthquake hazard research, *Eos Trans. AGU*, *79*(33), 393, 396–397.
Sauber, J., G. Plafker, B. F. Molnia, and M. A. Bryant (2000), Crustal deformation associated with glacial fluctuations in the eastern Chugach Mountains, Alaska, *J. Geophys. Res.*, *105*, 8055–8077.
Savage, J. C. (1983), A dislocation model of strain accumulation and release at a subduction zone, *J. Geophys. Res.*, *88*, 4984–4996.
Savage, J. C., and M. Lisowski (1988), Deformation in the Yakataga seismic gap, southern Alaska, 1980–1986, *J. Geophys. Res.*, *93*, 4731–4744.
Savage, J. C., and G. Plafker (1991), Tide gage measurements of uplift along the south coast of Alaska, *J. Geophys. Res.*, *96*, 4325–4335.
Savage, J. C., J. L. Svarc, and W. H. Prescott (1999), Deformation across the Alaska-Aleutian Subduction Zone near Kodiak, *Geophys. Res. Lett.*, *26*, 2117–2120.
Scholz, C. (1990), *The Mechanics of Earthquakes and Faulting*, 437 pp., Cambridge Univ. Press, New York.
Smith, W. H. F., and D. T. Sandwell (1997), Global sea floor topography from satellite altimetry and ship depth soundings, *Science*, *277*, 1956–1962.
Stockman, S., J. Sauber, and E. Linscheid (1997), A high school and NASA join forces to investigate the Alaska-Aleutian subduction zone near Kodiak Island, *J. Geosci. Educ.*, *45*, 440–446.
Taylor, M. A. J., G. Zheng, J. R. Rice, W. D. Stuart, and R. Dmowska (1996), Cyclic stressing and seismicity at strongly coupled subduction zones, *J. Geophys. Res.*, *101*, 8363–8381.
vonHuene, R., D. Klaeschen, and J. Fruehn (1999), Relation between the subducting plate and seismicity associated with the great 1964 Alaska earthquake, *Pure Appl. Geophys.*, *154*, 575–591.
Wahr, J., and M. Wyss (1980), Interpretation of postseismic deformation with a viscoelastic relaxation model, *J. Geophys. Res.*, *85*, 6471–6477.
Wells, R. E., R. J. Blakely, Y. Sugiyama, D. W. Scholl, and P. A. Dinterman (2003), Basin-centered asperities in great subduction zone earthquakes: A link between slip, subsidence, and subduction erosion?, *J. Geophys. Res.*, *108*(B10), 2507, doi:10.1029/2002JB002072.
Zheng, G., R. Dmowska, and J. R. Rice (1996), Modeling earthquake cycles in the Shumagin subduction segment, Alaska, with seismic and geodetic constraints, *J. Geophys. Res.*, *101*, 8383–8392.
Zweck, C., J. T. Freymueller, and S. C. Cohen (2002), Three-dimensional elastic dislocation modeling of the postseismic response to the 1964 Alaska earthquake, *J. Geophys. Res.*, *107*(B4), 2064, doi:10.1029/2001JB000409.

G. Carver, Department of Geology, Humboldt State University, Arcata, CA 95521, USA.
S. Cohen and J. Sauber, Planetary Geodynamics Laboratory, NASA's Goddard Space Flight Center, Code 921, Greenbelt, MD 20771, USA. (jeanne.m.sauber-rosenberg@nasa.gov)
R. King, Department of Earth, Atmospheric, and Planetary Science, Massachusetts Institute of Technology, Cambridge, MA 02139, USA.